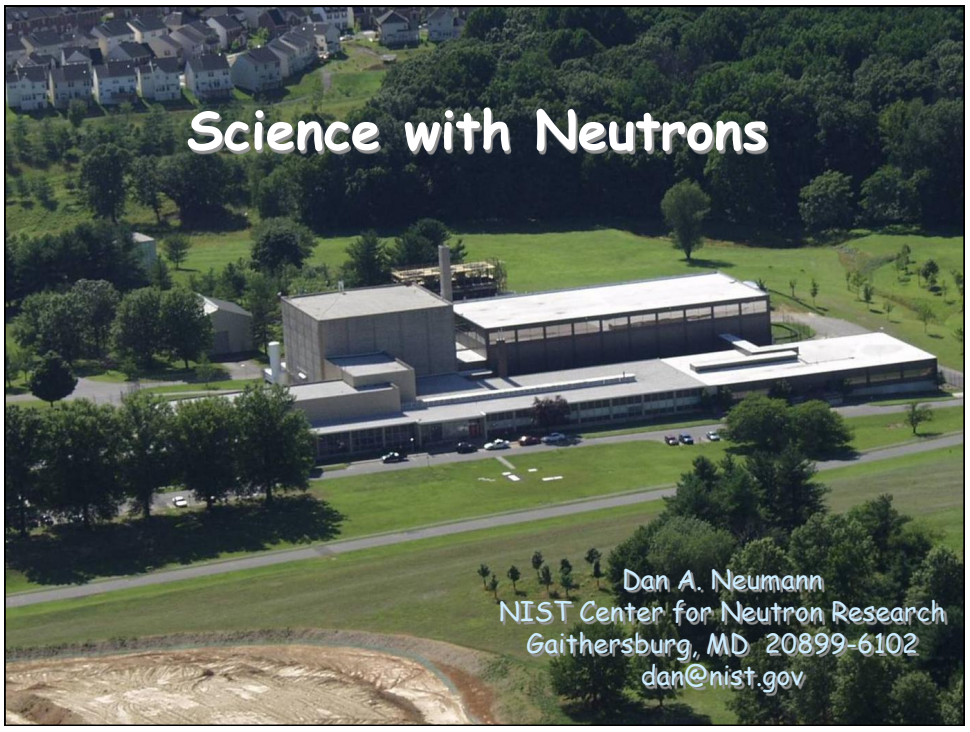

NIST Develops & Operates Neutron Instrumentation

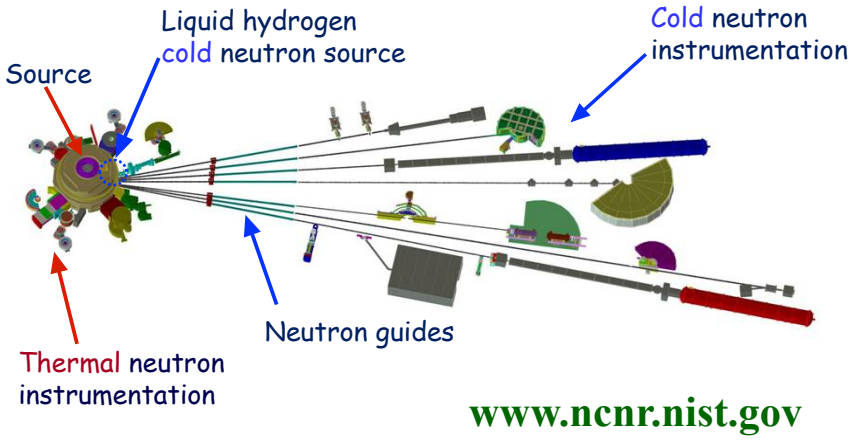

www.ncnr.nist.gov

Neutron scattering is an intensity limited technique
=> different instruments for different purposes

NIST

Techniques for the Measurement of Structure

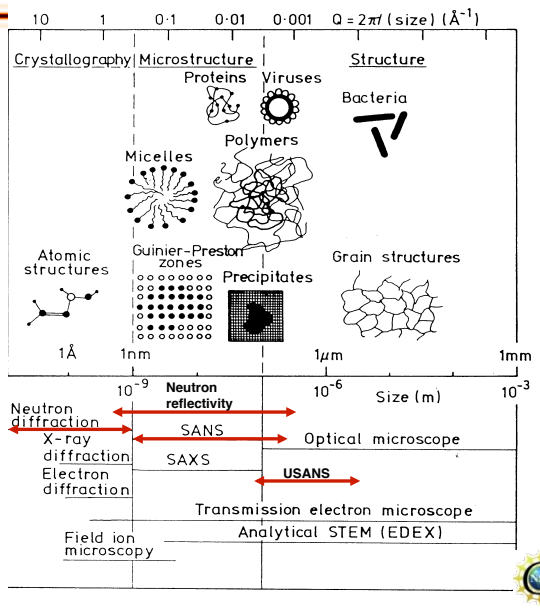

Diffraction Probes Structure in the Direction of Q

$$\vec{k}_i - \vec{k}_f = \vec{Q}$$

Specular Reflection Geometry

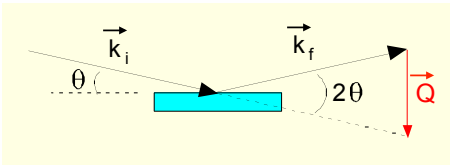

Reflectivity probes structure perpendicular to surface (parallel to Q), and *averages over structure in plane of sample.*

SANS Geometry

SANS probes structure in the plane (parallel to Q), and *averages over structure perpendicular to sample surface.*

Solving Multi-Phase Structures

Contrast Matching - reduce the number of phases "visible"

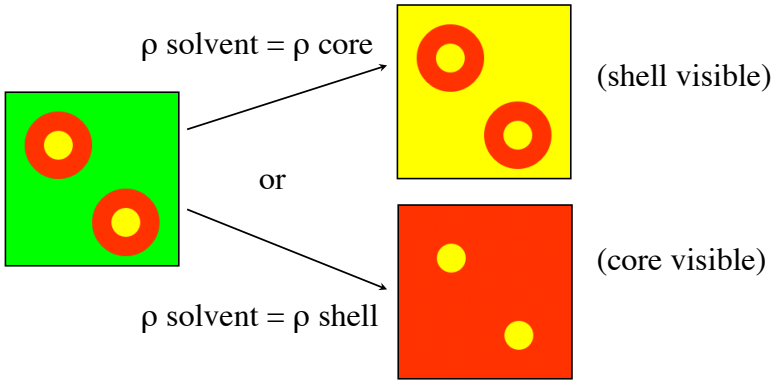

The two distinct 2-phase systems can be easily understood

NIST

Polymers

All commercially important polymers are immiscible.

1) The blending of polymers to achieve desired properties is restricted.

2) The recycling of most commingled plastic waste is precluded.

One can select block copolymers that stabilize blends of even highly immiscible polymers by acting as a "surfactant". This is accomplished by choosing the block copolymer so that it balances the attractive and repulsive interactions between the copolymer and the A-rich and B-rich phases.

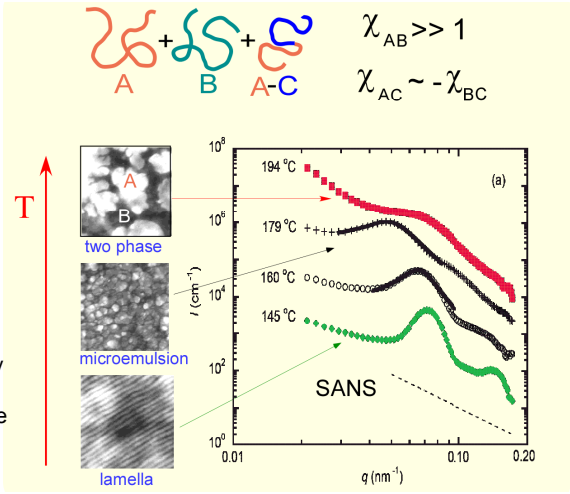

M.L. Ruegg *et al*., Macromolecules **39**, 1125 (2006).

CHRNS

Mesoporous Organohydrogels

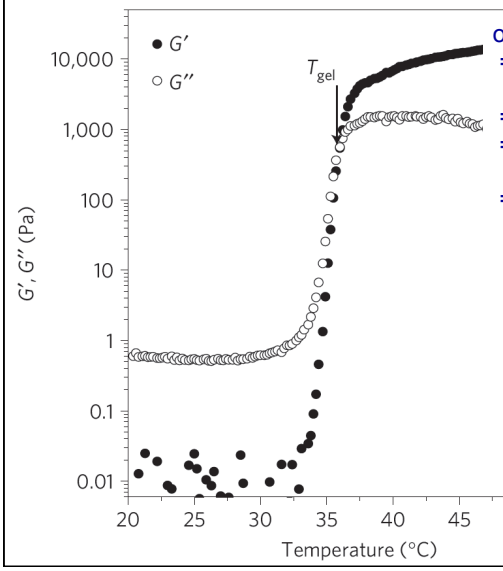

oil-in-water nanoemulsions
=> silicone oil (PDMS) droplets
[polydimethylsiloxane, (PDMS)]
=> aqueous continuous phase [18% D_2O]
=> functionalized hydrophilic polymer
[poly(ethylene glycol) diacrylate (PEGDA)]
=> surfactant (SDS)

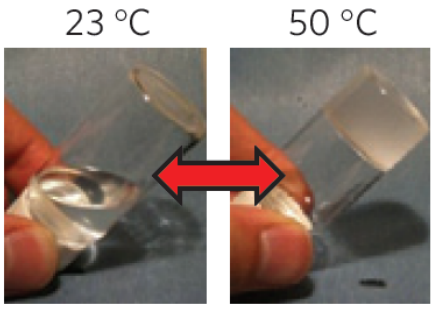

Mechanism of Organohydrogel Formation

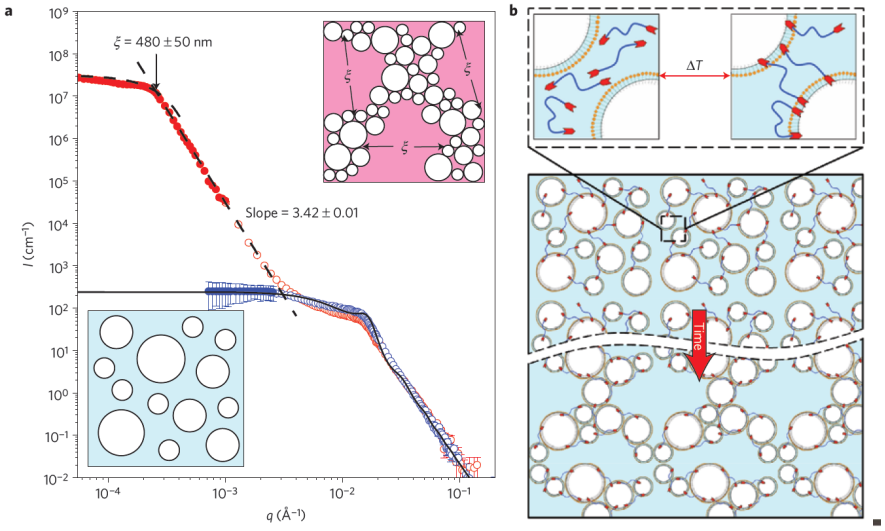

M.A. Helgeson, *et al.*, Nature Materials **11**, 344 (2012)

After Photcrosslinking

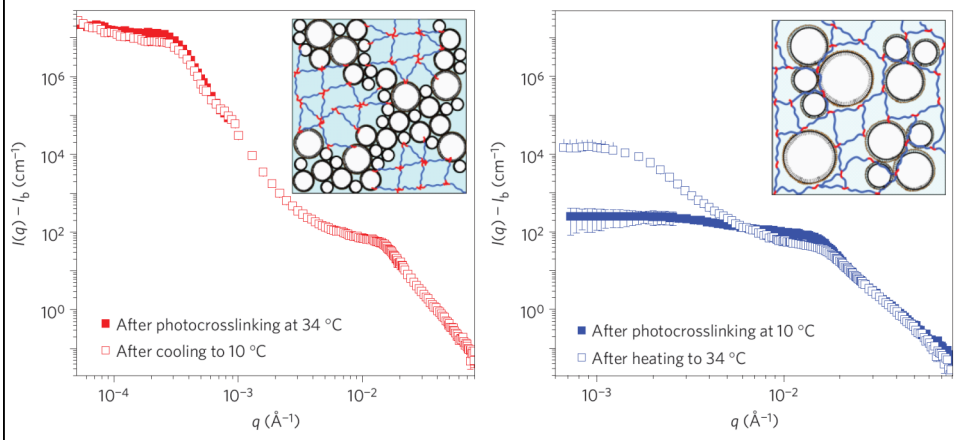

M.A. Helgeson, *et al.*, Nature Materials **11**, 344 (2012)

Polymer-SWNT Nanocomposites

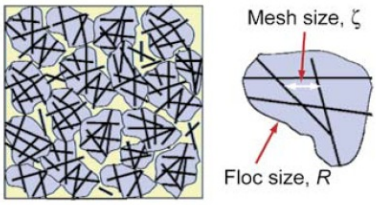

Network →Flocs (R)→ Mesh (ζ)→Single tube

R ≈ 4μm independent of concentration

SWNT's dispersed in polymer nanocomposites creates a percolated network structure above p_c

Scaling indicates a hierarchical network structure over a wide range of length scales

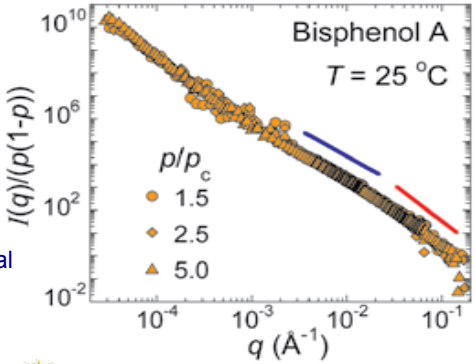

T Chatterjee, A. Jackson, R. Krishnamoorti, J. Am. Chem. Soc. **130**, 6934 (2008)

Polymer-SWNT Nanocomposites

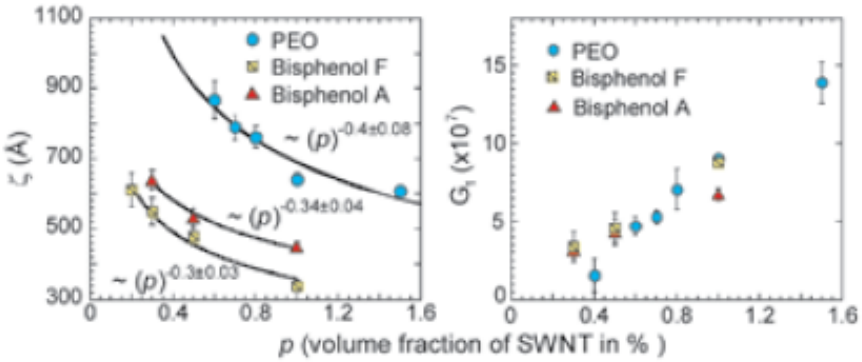

Weak mesh scaling can not explain the observed scaling exponent

The interactions between flocs (either directly or mediated by polymer), control the scaling dependence of the elastic strength of the network

T Chatterjee, A. Jackson, R. Krishnamoorti, J. Am. Chem. Soc. **130**, 6934 (2008)

Organic Solar Cells

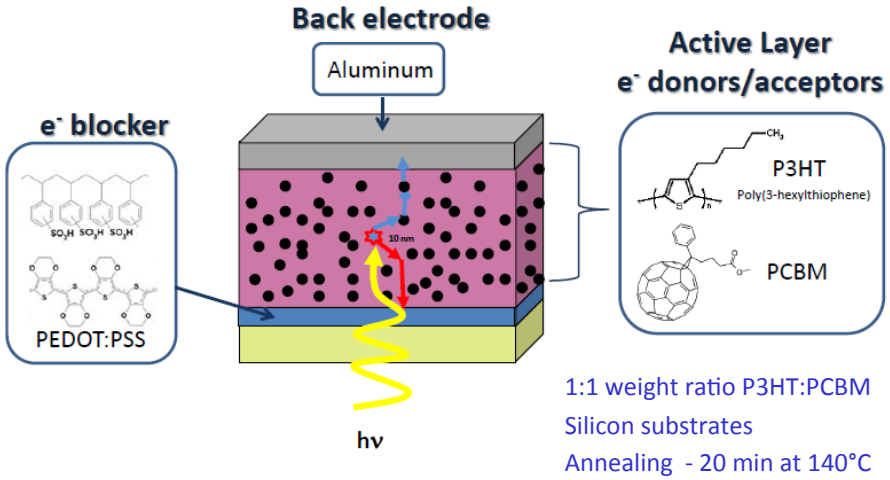

1:1 weight ratio P3HT:PCBM

Silicon substrates

Annealing - 20 min at 140°C

J. Kiel, B.J. Kirby, C. Majkrzak, B. Maranville, and M. Mackay, submitted.

Neutron Reflectivity

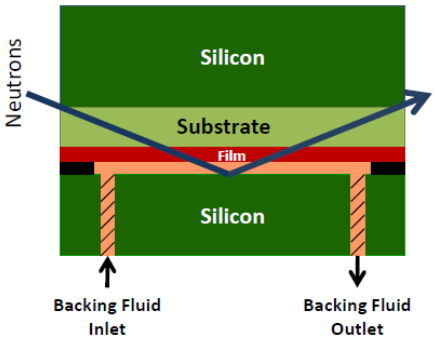

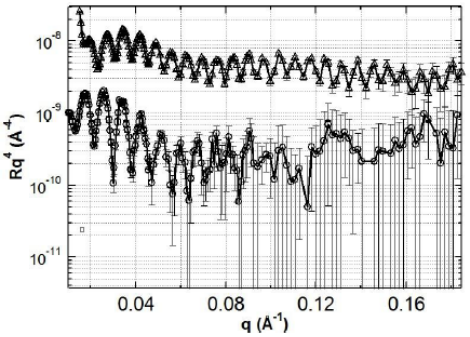

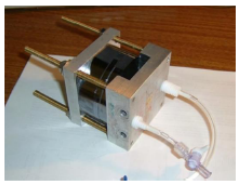

Addition of high SLD backing media greatly enhances scattering intensity and statistics

J. Kiel, *et al.*, Soft Matter **6**, 641 (2010)

Dispersion of PCBM

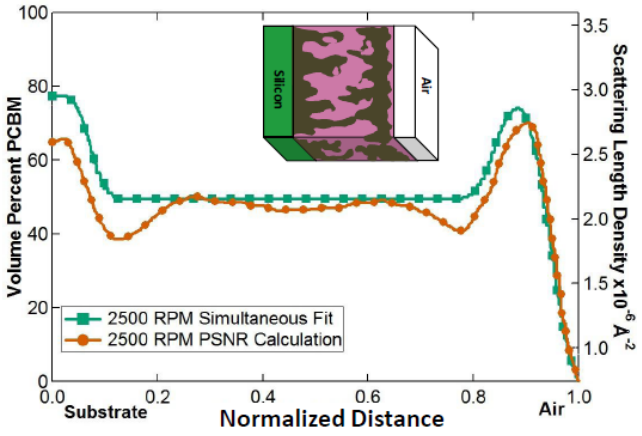

- Simultaneous fitting and PSNR calculations show agreement
- High PCBM concentration at substrate
- High PCBM concentration near air interface

J. Kiel, *et al.*, Soft Matter **6**, 641 (2010)

Effect of Annealing

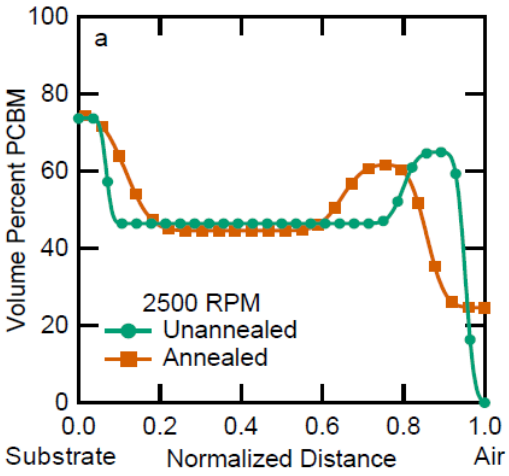

- Silicon substrate with 40 nm PEDOT:PSS
- Annealed 140°C for 20 minutes
- PCBM concentration increases from 0.2% to 25% at air interface
- Energy conversion efficiency increases by a factor of 4

J. Kiel, *et al.*, Soft Matter **6**, 641 (2010)

Phospholipid Membranes

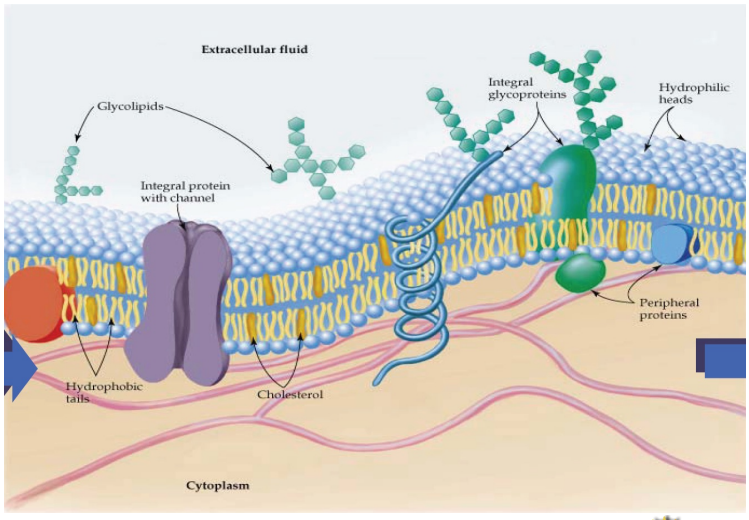

Tethered Bilayer Membranes (tBLM)

Bio-mimetic environment for studying protein-lipid interactions
(developed at NIST)

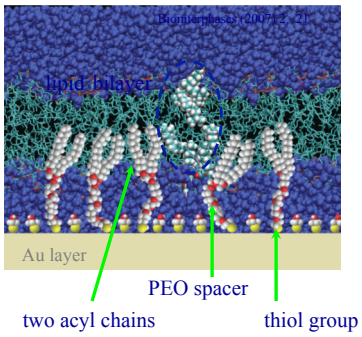

- Tether partially decouples bilayer from substrate
- Accommodate Proteins with sub-membrane domains
- Fluid bilayer is highly stable
  - Data acquisition times of several days
  - Resilient to exchange of aqueous phase
  - In situ sample manipulation

α-hemolysin in a Biomimetic Membrane

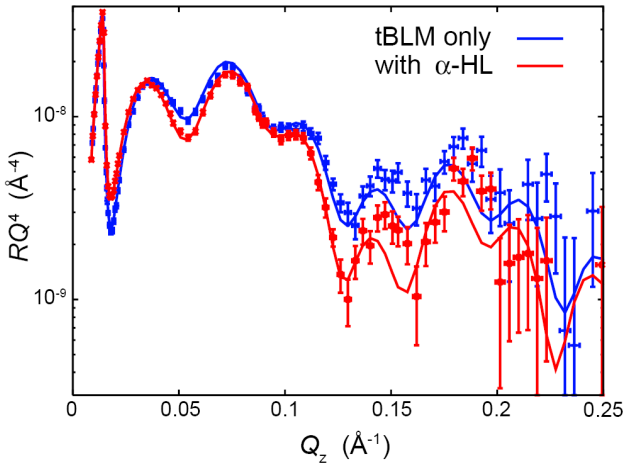

Toxins sometimes kill cells by forming pores in the cell membrane.

α-hemolysin (αHL) is a toxin produced by *Staphylococcus aureus.*

D.J. McGillivray, *et al.*, Biophys. J. **96**, 1547 (2009).

α-hemolysin in a Biomimetic Membrane

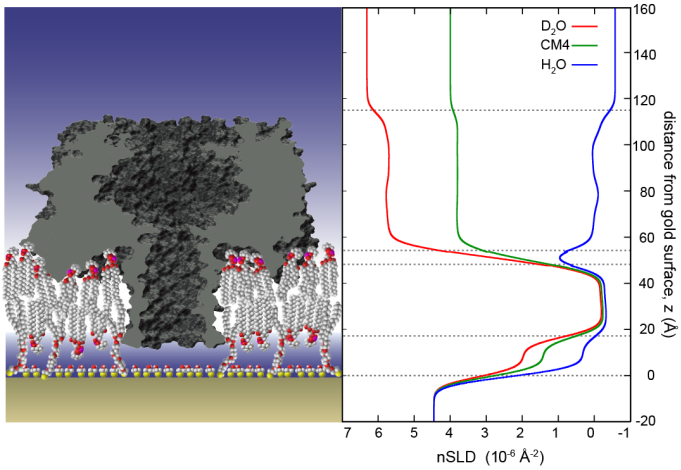

The protein rim is seen to interact strongly with the lipid headgroups.

The crystal structure of the toxin was used in the fits.

D.J. McGillivray, *et al.*, Biophys. J. **96**, 1547 (2009).

Tethered Bilayer Membranes (tBLM)

Bio-mimetic environment for studying protein-lipid interactions
(developed at NIST)

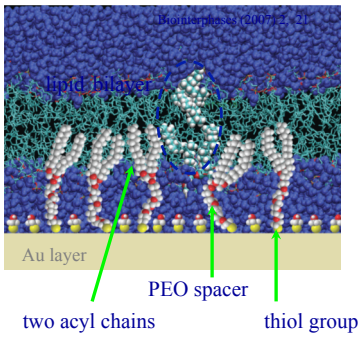

- Tether partially decouples bilayer from substrate
- Accommodate Proteins with sub-membrane domains
- Fluid bilayer is highly stable
  - Data acquisition times of several days
  - Resilient to exchange of aqueous phase
  - In situ sample manipulation

Basic Structure of an Immature Retrovirus

Biochemical evidence suggests that HIV-1 Gag is NOT extended in solution.

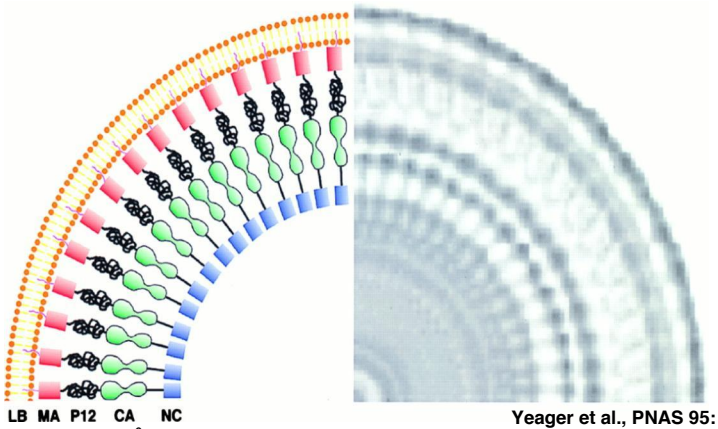

Yeager et al., PNAS 95: 7299, 1998

Mimicking the Viral Lipidome

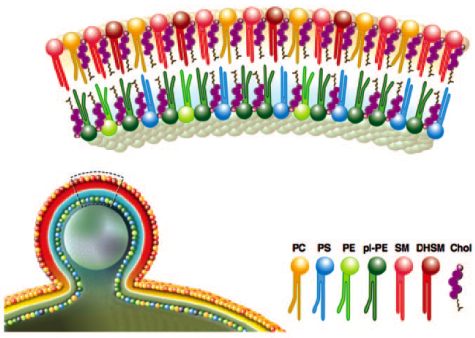

Lipid bilayer composition chosen to mimic viral lipidome:

- d_{54} -DMPC (d-DMPC, zwitterionic)
- DMPS (anionic, increases electrostatic interactions
- Cholesterol

d-DMPC:DMPS:Cholesterol = 70:30:3 produced the most complete bilayer

Modeling the Gag Protein Layer

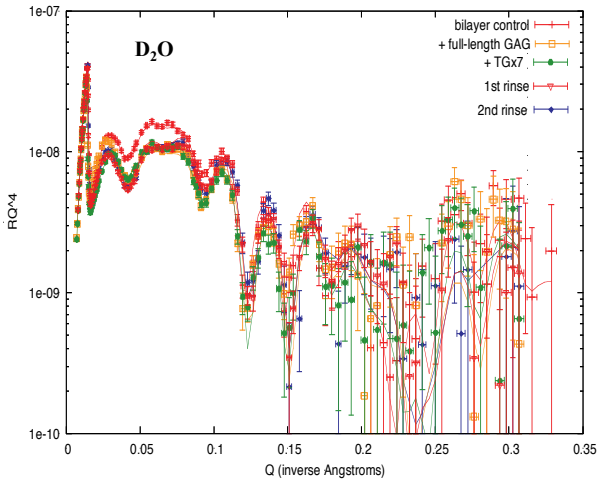

SLD profiles determined by simultaneous fitting of **13** measurements:

- Three contrasts (D_2O, H_2O and CM4) for
- Bilayer control
- Gag Binding
- Gag + TG14 DNA
- Rinse 1: 250 mM NaCl

- Rinse 2: 500 mM NaCl only measured in D_2O

H. Nanda, *et al*., Biophys. J. (2010).

Gag Layer On Membrane Surface

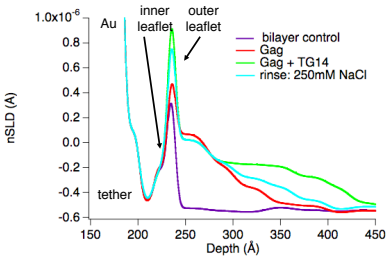

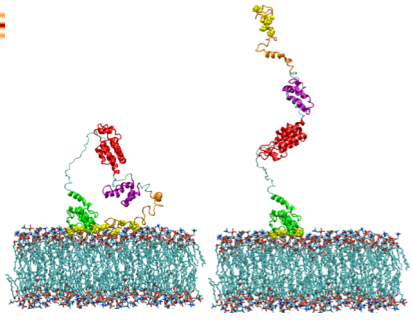

nSLD increases for distances beyond the lipid bilayer surface.

nSLD increases at greater distances from the lipid bilayer surface.

High salt rinse removes DNA and original profile is recovered.

H. Nanda, *et al*., Biophys. J. (2010).

Model for Gag Assembly on Bilayer

Both nucleic acid and lipid binding
are needed for extension of Gag protein

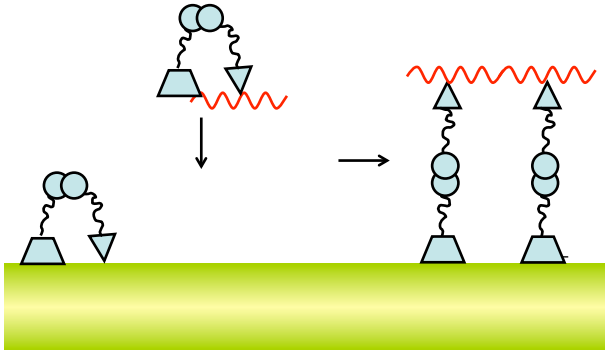

H. Nanda, *et al*., Biophys. J. (2010).

Neutron Spin Echo

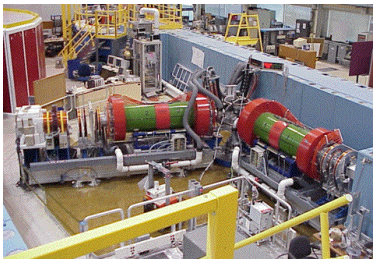

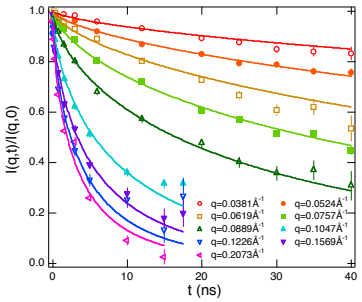

I(q,t); space-time correlation function between an object existing at time t and that existed at t=0.

$$I(q,t) = \int G(r,t)\exp(iqr)dr$$

$$= \int S(q,\omega)\exp(i\omega t)d\omega$$

$$I(q,0) = \int S(q,\omega)\exp(0)d\omega = \int S(q,\omega)d\omega$$

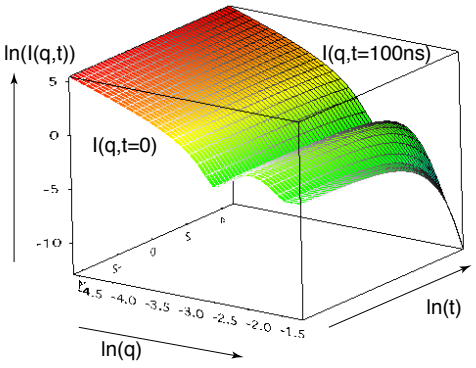

Thickness Fluctuations in a Surfactant Membrane

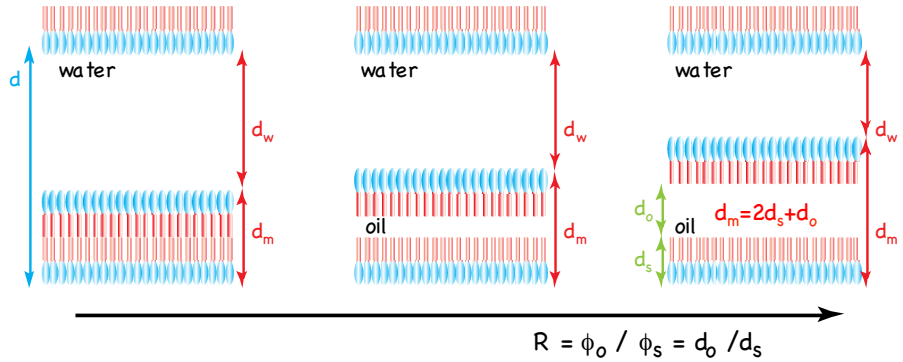

Surfactant bilayers are swollen by oil. The dynamics change due to the increase of the bilayer thickness has been investigated as a function of $R=\phi_o/\phi_s$.

Experiment

Sample: $C_{12}E_5/D_2O/C_8D_{18}$ (C_8H_{18}) ϕ_{C12E5}=constant $R=\phi_{C8D18}/\phi_{C12E5}$=variable

NIST

Q-dependence of the Relaxation Rate

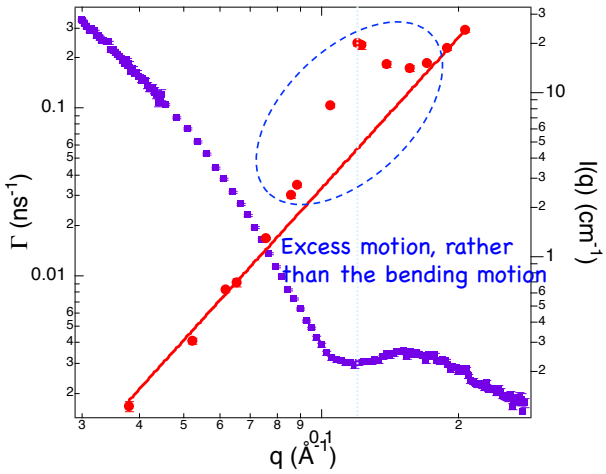

Thickness fluctuations in the swollen lamellar phase

Excess dynamics observed at the q-range, where the dip in SANS profile.

The dip in SANS corresponds to the length scale of the membrane thickness.

M. Nagao, PRE **80**, 031606 (2009).

CHRNS

Comparison with MD Simulation

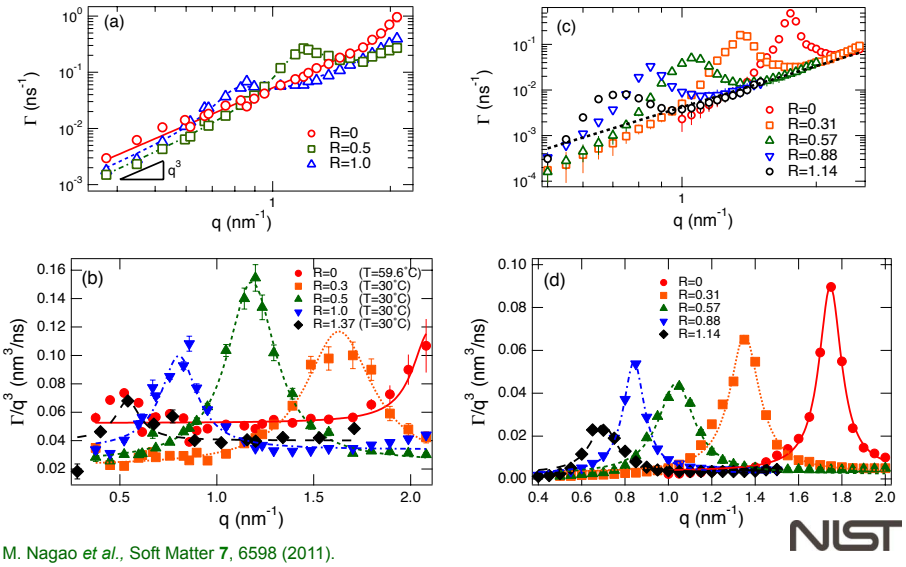

M. Nagao *et al.*, Soft Matter **7**, 6598 (2011).

Amplitude of the Thickness Fluctuations

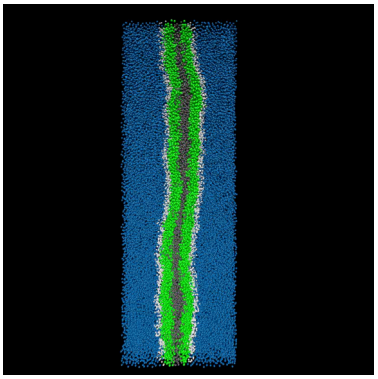

Thickness fluctuation amplitude

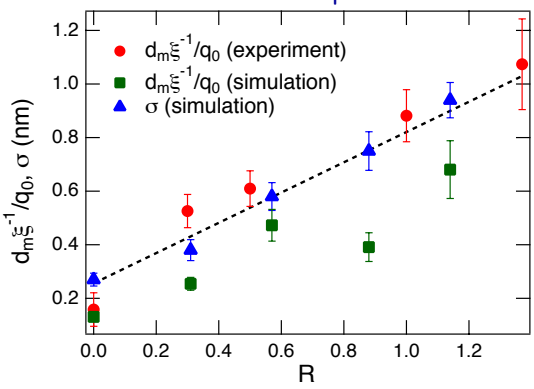

Good agreement.
Amplitude is about 12% of membrane thickness

M. Nagao *et al., Soft Matter* **7**, 6598 (2011).

Expansion Activities

- New Cold Source
- Construction
- Instrument development
- Beam delivery
- Reactor reliability enhancements

NIST

NCNR Expansion

Many sub-projects:

5 new capabilities
MACS relocation
instrument moves
software
guides/shields
cold source

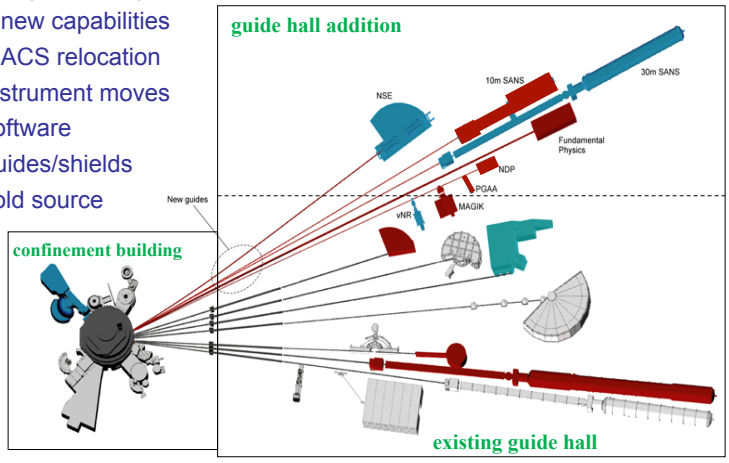

Major areas of activity:

Construction
Cold source
Guide systems
Shield systems
Instruments
Control room upgrade

NIST

Roughly the Current Situation

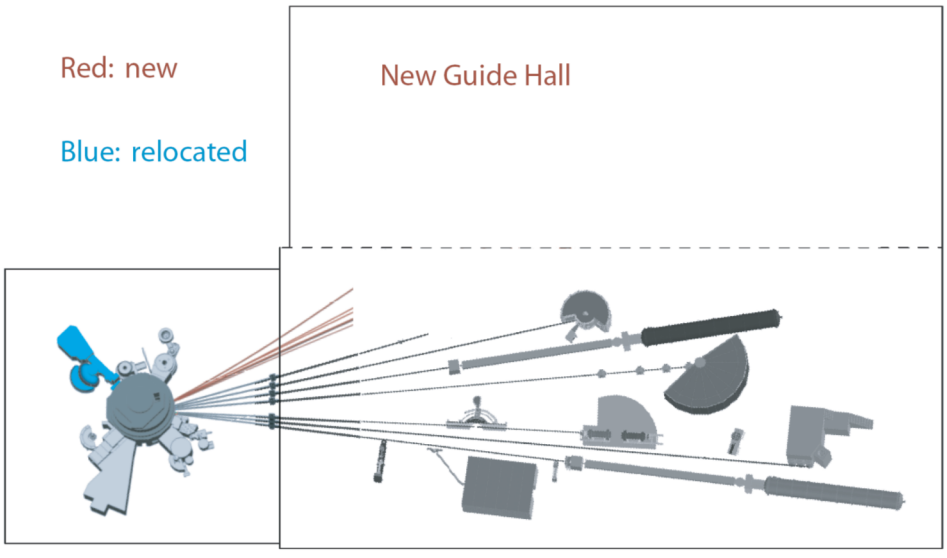

Eventual Configuration

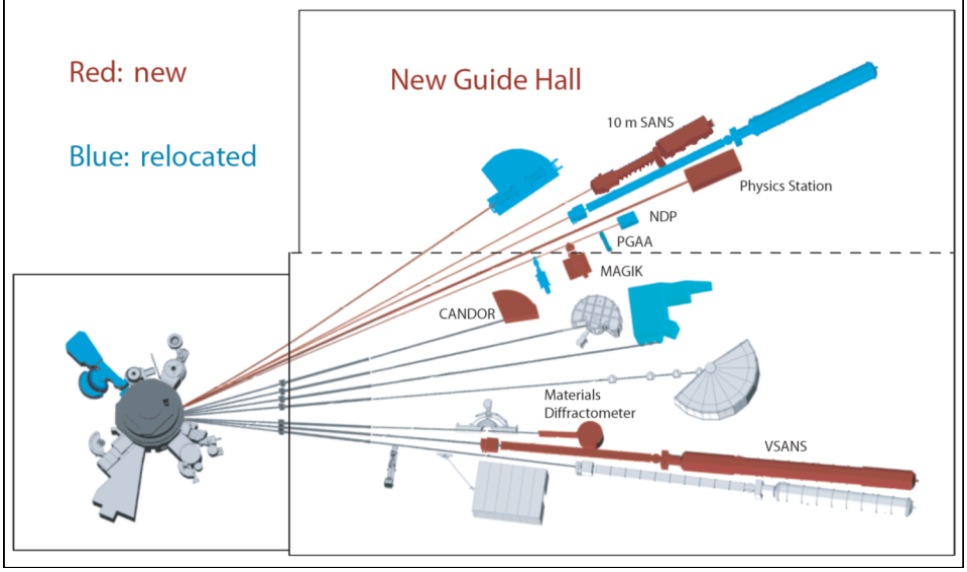

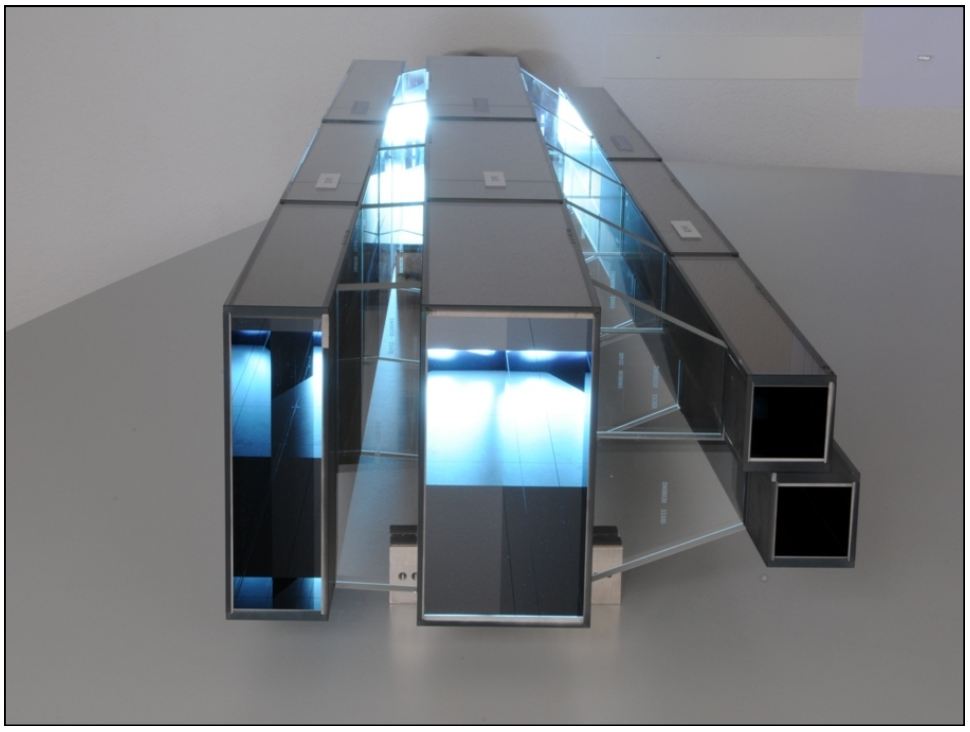


8450 lbs

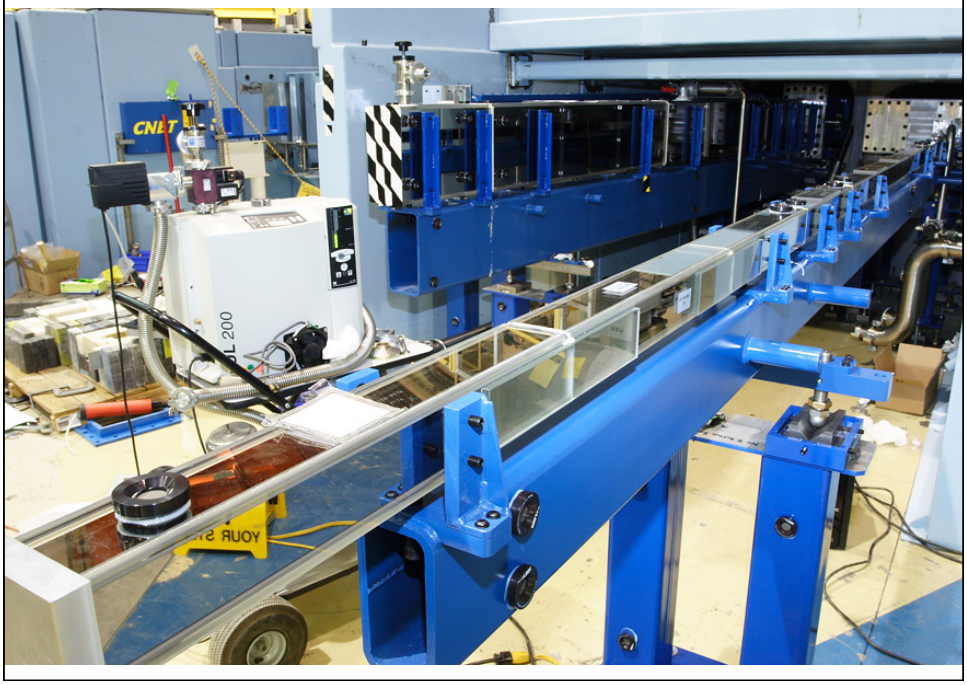

MAGIk

We can **increase intensity** by using **multiple** beams to reduce measuring time.

Suppose that we have **N incident beams** that can be **tagged at will**. Various tagging strategies are being considered.

A second way to gain: a **Position Sensitive Detector** (PSD) permits **parallel processing** to reduce the measuring time: each pixel is simultaneously recording data. Below, **consider one pixel** of the PSD.

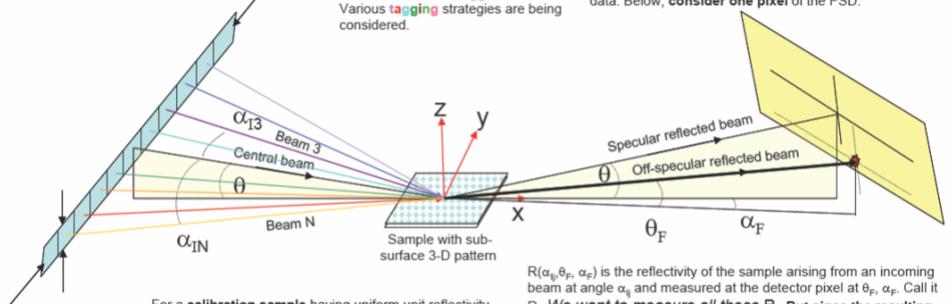

The slit is narrow along z to fix θ, but **broad along y** to gain Intensity.

For a **calibration sample** having uniform unit reflectivity, R = 1, the contribution, M, of each beam to the signal at the detector pixel for each tagging condition must be measured separately.

$R(\alpha_i, \theta_F, \alpha_F)$ is the reflectivity of the sample arising from an incoming beam at angle α_i and measured at the detector pixel at θ_F, α_F. Call it R_i. *We want to measure all these* R_i. **But since the resulting signal contains the SUM of terms arising from each incident beam, the terms need to be separated.** By using a number of tagging conditions and measuring once for each condition, this separation can be accomplished.

NIST

Off-specular neutron reflectometry

For patterned films

- probes length scales larger than SANS

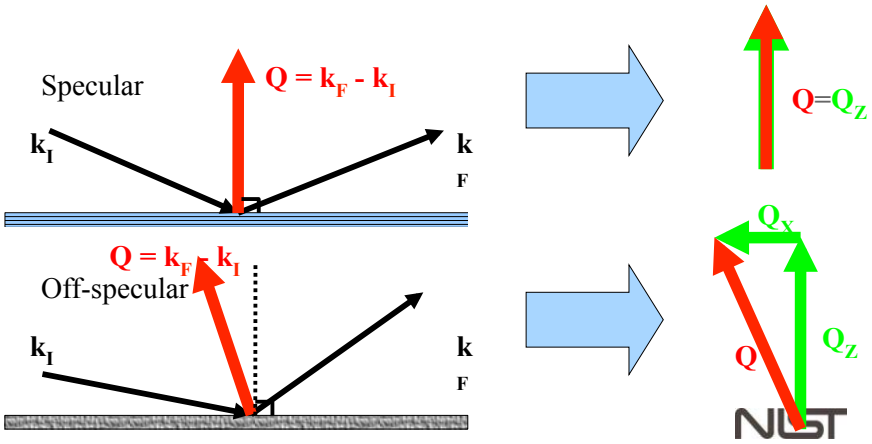

CANDoR

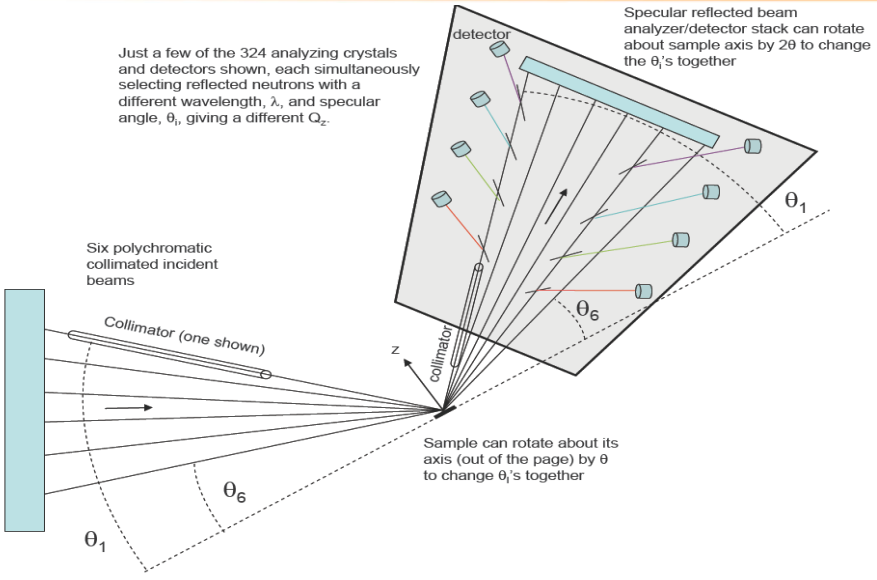

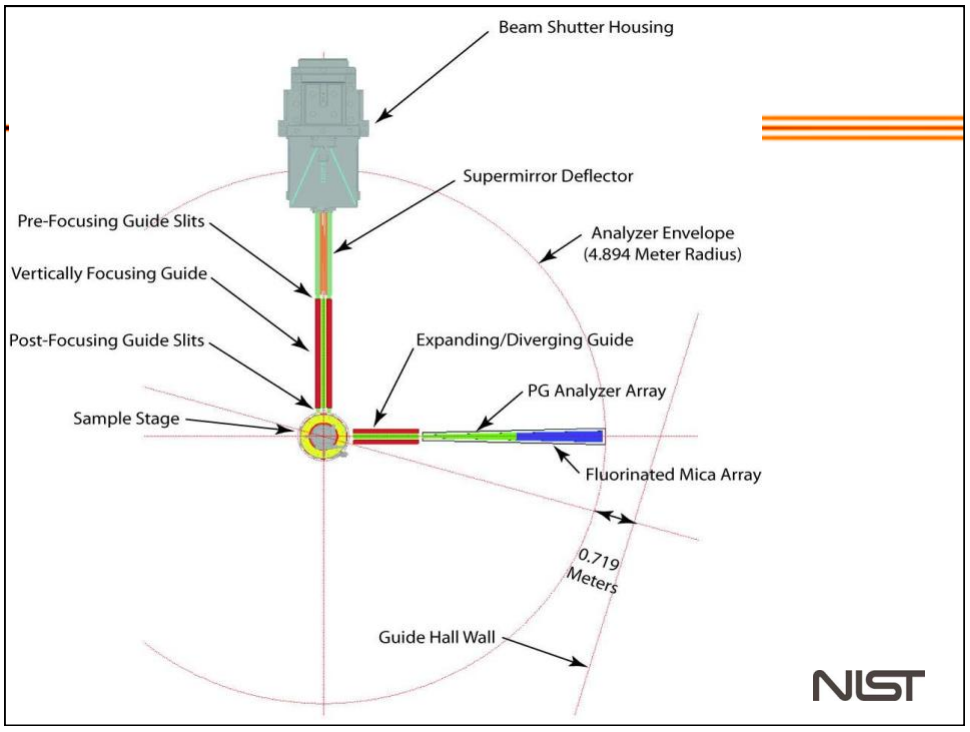
Beam Shutter Housing
Supermirror Deflector
Pre-Focusing Guide Slits
Analyzer Envelope
(4.894 Meter Radius)
Vertically Focusing Guide
Post-Focusing Guide Slits
Expanding/Diverging Guide
PG Analyzer Array
Sample Stage
Fluorinated Mica Array
0.719
Meters
Guide Hall Wall
NIST

CANDoR

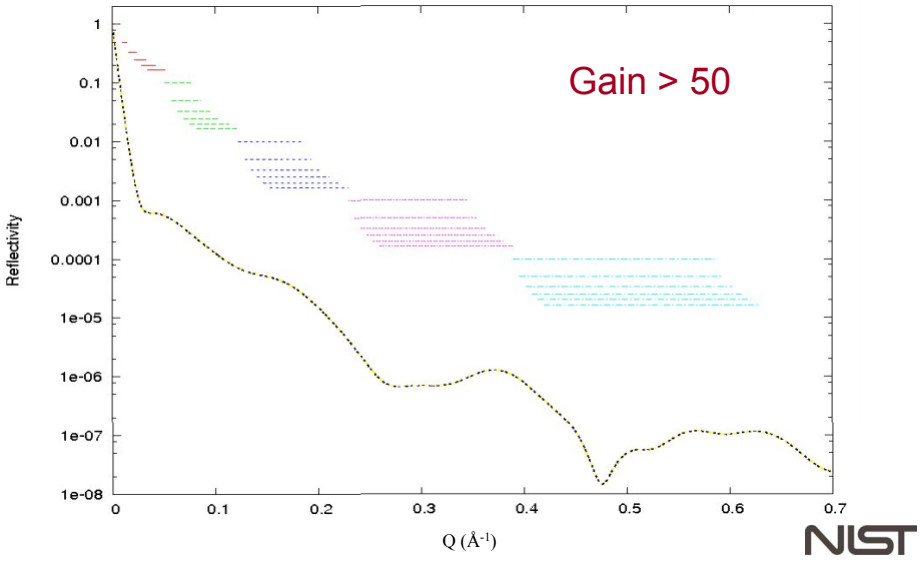
Gain > 50
Reflectivity
1
0.1
0.01
0.001
0.0001
1e-05
1e-06
1e-07
1e-08
0
0.1
0.2
0.3
0.4
0.5
0.6
0.7
Q (Å-1)
NIST

Why vSANS?

Extends the q-range of the 30 m SANS instruments to enable most SANS experiments to be completed on one instrument

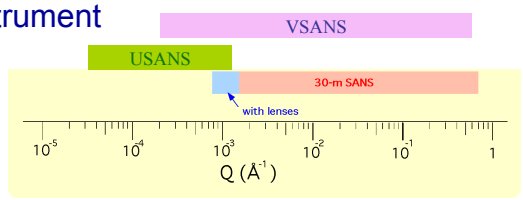

- 2% or 13.5 % wavelength band
- expandable sample staging area
- multiple detectors to extend q-range of a single measurement
- improved polarization analysis

NIST

vSANS

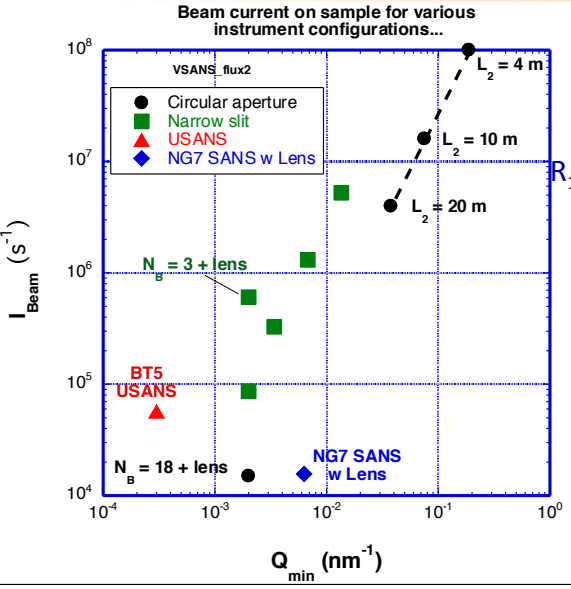

Multiple Circular Beams

R_1 = 3 mm, R_2 = 5 mm, λ = 8.5 Å

Lens gain ~ $(5/1.5)^2$ = 11

beams gain = 18

Total Gain = 200

NIST

vSANS – Refractive Optics

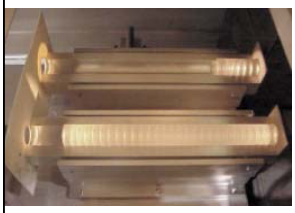

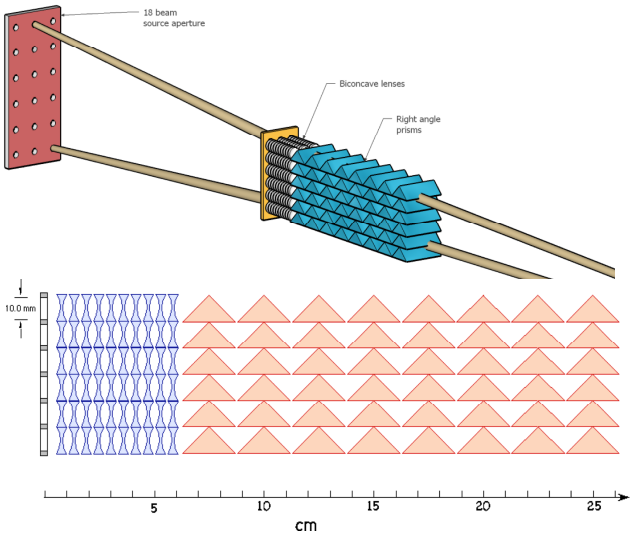

vSANS

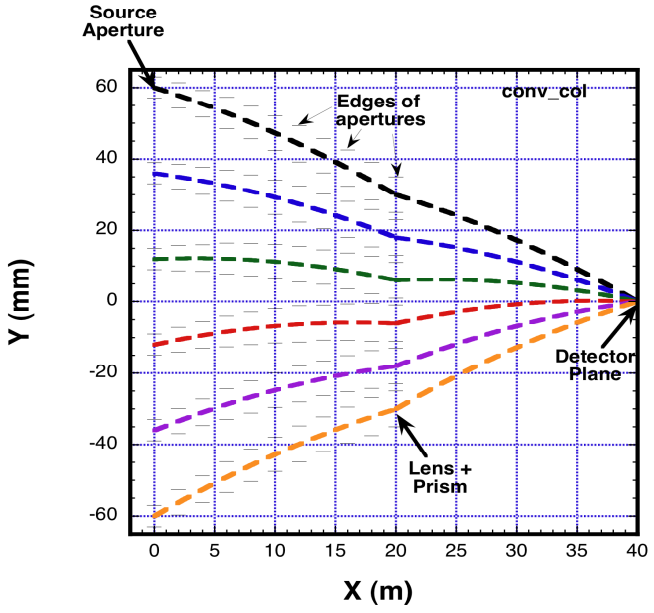

vSANS – Detector

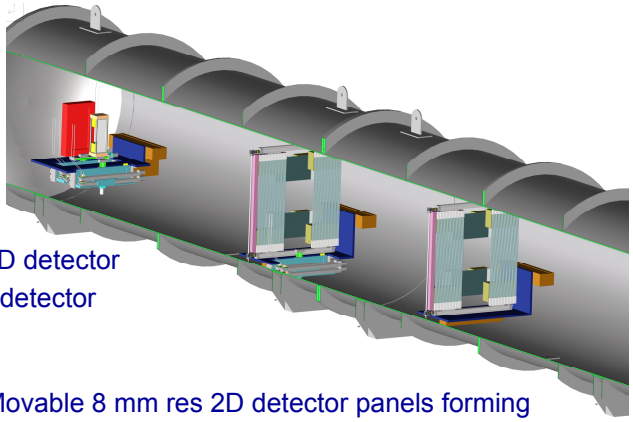

High res (1-2 mm) 2D detector
High res (1 mm) 1D detector

Movable 8 mm res 2D detector panels forming
1 m^2 area on front and middle carriage

NIST

10 Low-Q Instruments

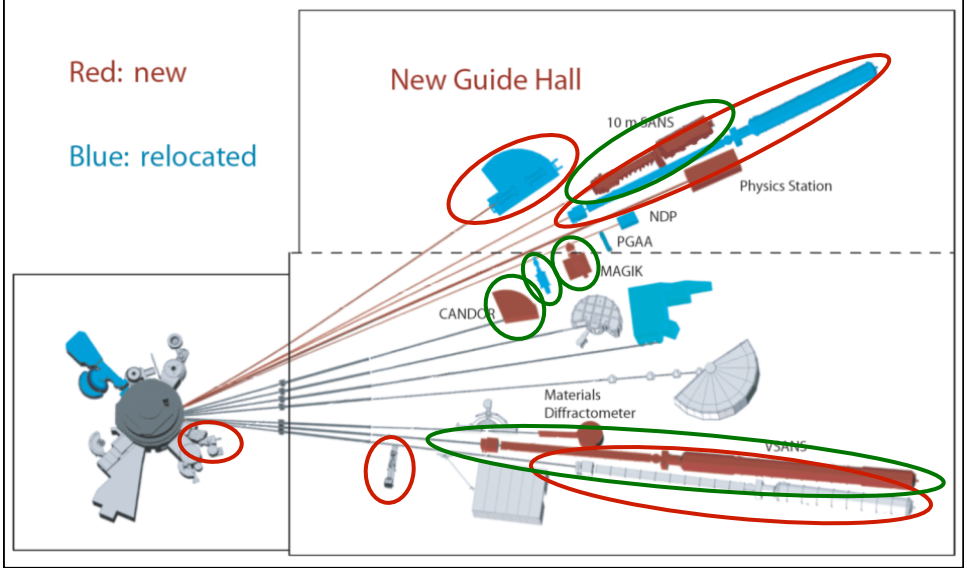

Block Co-polymer in a Si Grating

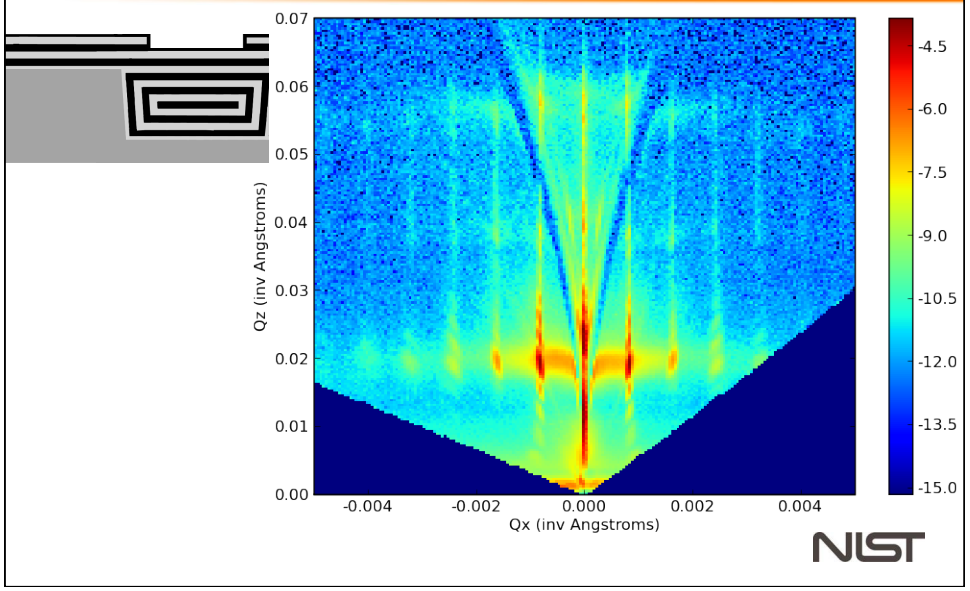

Block Co-polymer in a Si Grating

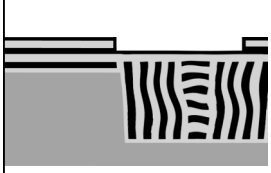

More vertically aligned lamellae

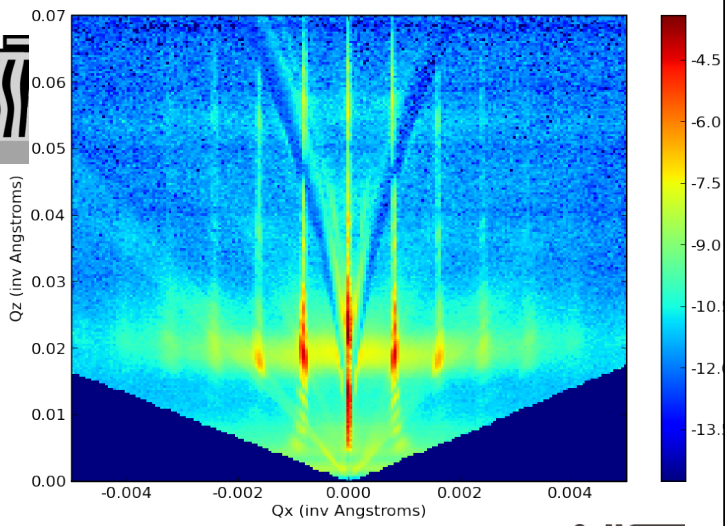

NIST

Block Co-polymer in a Si Grating

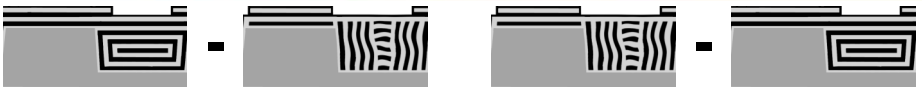

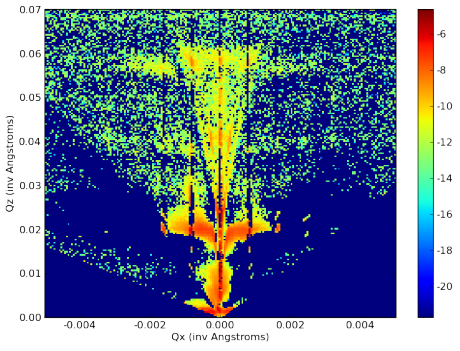

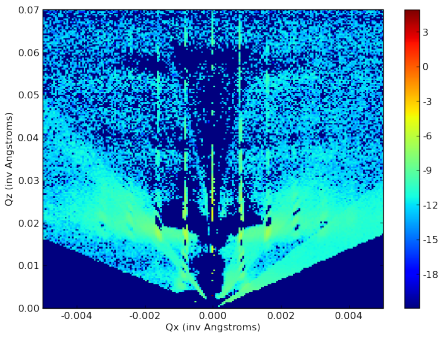

Stronger scattering near Q_x=0, and at high Q_z

Stronger at high Q_x

NIST